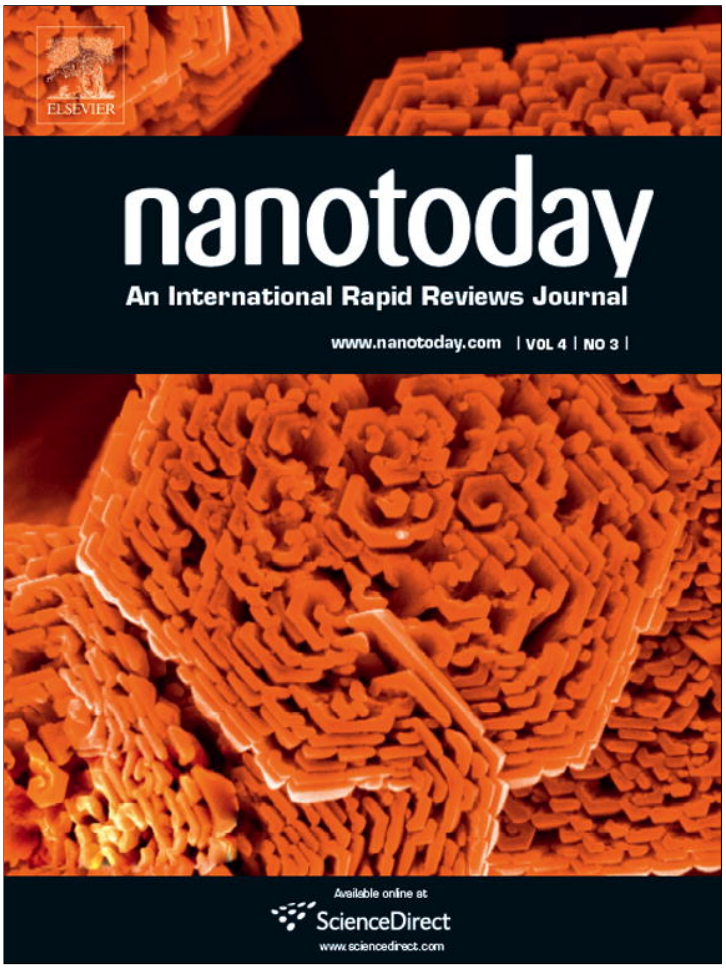

Nano Today (2009) 4, 269—279

available at www.sciencedirect.com

ScienceDirect

journal homepage: www.elsevier.com/locate/nanotoday

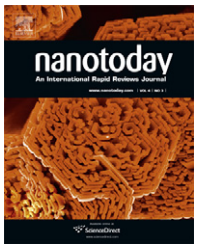

REVIEW

Spectroscopy in sculpted fields

Nan Yang[a], **Yiqiao Tang**[b], **Adam E. Cohen**[b,*]

[a] *School of Engineering and Applied Science, Harvard University, United States*
[b] *Department of Physics, Harvard University, United States*

Received 2 April 2009; received in revised form 1 May 2009; accepted 1 May 2009

KEYWORDS
SERS;
SEROA;
Chirality;
Superhelical light;
Intersystem crossing;
Magnetic field effect

Summary Metallic and magnetic nanostructures set electromagnetic boundary conditions which can lead to highly contorted fields in their immediate vicinity. While much attention has been devoted to enhancements in electric field *strength*, we argue that equally interesting phenomena arise from enhancements in magnetic and electric field *gradients*. Nonuniform fields near nanostructures can induce molecular transitions that are forbidden by electric dipole selection rules. We illustrate this claim with two examples. ''Superhelical'' electromagnetic fields are predicted to show enhanced asymmetry in their interaction with chiral molecules, far greater than that due to circularly polarized light. Such fields could be used to induce chiral photochemistry with large enantiomeric excess. Steeply varying DC magnetic fields are predicted to enhance the rate of intersystem crossing in molecular bi-radicals. Such fields could provide a route to new nanomagnetic catalysts and to magnetic control of chemical reactions.

Introduction

Recent progress in nanotechnology has led to qualitatively new ways to study and to control light—matter interactions. Metallic and magnetic nanostructures allow one to sculpt the three-dimensional shape of the electromagnetic field on the size scale of an individual molecule. These sculpted fields interact with the three-dimensional shape of a molecule to drive molecular transitions that would be tickled extremely weakly — if at all — by radiation from macroscopic sources. The prospect of spectroscopy in sculpted fields promises new insights into fundamental aspects of light—matter interactions, as well as new technological developments.

The purpose of this review is to develop a systematic approach to thinking about nano-optical effects in terms of the symmetries of the electromagnetic field and the molecules with which it interacts. Many known nano-optical effects can be classified by the symmetries of the enhanced fields. We illustrate the utility of this classification scheme with two recent predictions for nano-optical phenomena:

(a) excitation of a single chiral enantiomer in the presence of its mirror-image brethren, with an enantioselectivity hundreds of times larger than that of circularly polarized light and
(b) creation of photochemical reactions where the outcome is exquisitely sensitive to proximity to a magnetic nanostructure.

* Corresponding author at: Department of Chemistry and Chemical Biology, Harvard University, 12 Oxford Street, Cambridge, MA 02138, United States. Tel.: +1 617 496 9466; fax: +1 617 495 9131.
E-mail address: cohen@chemistry.harvard.edu (A.E. Cohen).

1748-0132/$ — see front matter
doi:10.1016/j.nantod.2009.05.001

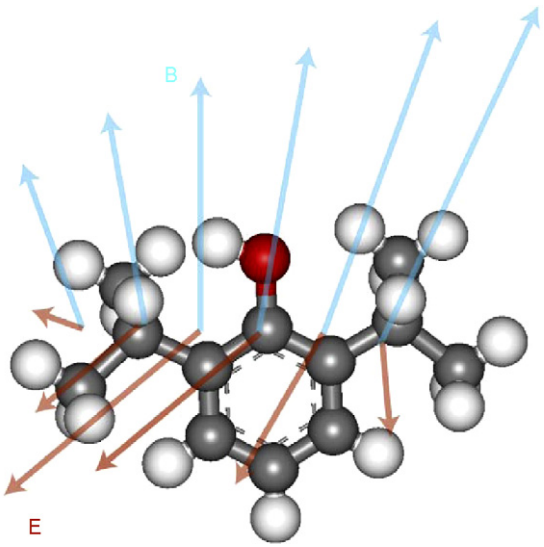

Figure 1 Spectroscopy in sculpted fields. In this schematic illustration, a molecule experiences electric and magnetic fields that vary over the size of the molecule. The fields at each point in the molecule may be complex functions of time.

An ultimate goal of spectroscopy is to control the electromagnetic field throughout a complex molecule, atom-by-atom and femtosecond-by-femtosecond (Fig. 1) [1,2]. The goal of ultrafast spectroscopy is to change the field on timescales comparable to the internal dynamics of a molecule, and thereby to learn about these dynamics [3]. While there is much work on pushing spectroscopy to femtoseconds and below, there is currently less emphasis on creating fields that vary significantly over distances comparable to the size of a molecule. Spatially engineered fields allow one to probe the physical structure of a molecule and its excitations in a manner that is inaccessible to far-field techniques working on any timescale, even ultrafast. These two approaches provide complementary information about the temporal and spatial dynamics of excitations within complex molecules. Eventually, spatial and temporal sculpting of electromagnetic fields will be combined to achieve the ultimate goal of full spatiotemporal control.

Molecular dark states

Molecules have a host of states that are only weakly coupled to, or simply invisible to, far-field radiation. This situation arises because the wavelength of plane waves of visible light ($\lambda \sim$400—700 nm) is vastly larger than the size of a typical molecule ($R_{mol} \sim$0.2—1 nm). Due to this size mismatch, the molecule ''sees'' uniform electric and magnetic fields, just as we see the Earth as locally flat.

Textbooks of spectroscopy typically take advantage of this size mismatch to make the ''point-dipole approximation'' (PDA), in which we assume that the electromagnetic field is perfectly uniform over the extent of the molecule. The PDA implies selection rules that govern which states can be reached via linear or nonlinear optical excitation. Dipole-forbidden transitions occur with probabilities smaller by powers of $R_{mol}/\lambda \sim 1/1000$ than dipole-allowed transitions. The small probability associated with these dipole-forbidden transitions means that under most conditions they may be neglected.

Yet in intermolecular processes the electromagnetic field due to one molecule may be highly nonuniform over the extent of a neighboring molecule, and thus ''forbidden'' transitions can play an important role. This statement is encapsulated within the multipole expansion of the intermolecular interaction. An arbitrary bounded distribution of charges and currents (e.g. a molecule) may be expanded as a series of multipoles, where the electric (or magnetic) field of the nth multipole falls off as $1/r^{n+2}$. A point charge corresponds to a multipole of order $n = 0$, a dipole to $n = 1$, a quadrupole to $n = 2$, and so on. Coupling of the nth multipole of molecule A to the mth multipole of molecule B yields an interaction energy that falls off as $(1/R_{AB})^{m+n+1}$. For neutral molecules at large separation, only the dipole—dipole term remains, and the usual selection rules apply. But when the intermolecular spacing becomes comparable to the molecular size — as often happens in condensed matter — higher multipole moments contribute significantly and the cherished selection rules of far-field spectroscopy are relaxed.

Dark states and forbidden transitions play an important role in mediating intermolecular energy transfer [4], intermolecular forces [5], and chemical reactions [6]. One can now imagine replacing one molecule by a metallic or magnetic nanostructure. Nanostructures can generate electric and magnetic fields with immense field gradients, at frequencies ranging from DC up to optical. Furthermore, the relative magnitude and direction of electric and magnetic fields near a nanostructure need not correspond with their values in a plane wave. These highly contorted electromagnetic fields are capable of enhancing electric dipole-forbidden transitions in nearby molecules.

Nano-enhanced optical effects

Surface-enhancement effects are well known for molecules near metal surfaces [7,8], and such effects can lead to dramatic enhancements in fluorescence [9] and Raman [10] signals. Plasmon enhancement effects have also been used to polymerize photoresist [11] and to induce nonlinear processes such as two-photon excitation [12]. These phenomena are typically interpreted in terms of enhancement of the field strength alone [7]; we are interested in using nanostructures to reshape the electric and magnetic fields and thereby to bring molecular dark states to light.

Table 1 provides a classification of the nano-enhanced optical transitions that have been either observed or predicted. Interesting and subtle effects arise from the enhancement of quantities other than the electric field strength. For instance, circular dichroism signals are enhanced for chiral molecules adsorbed near plasmonic nanoparticles [13,14]. Circular dichroism in randomly oriented molecules arises from an interference between electric dipole and magnetic dipole transitions, so the enhancement involves enhancement of both electric and magnetic fields. Enhanced Faraday rotation has also been predicted [15] and observed in magnetic nanoparticles [16,17] and nanohole arrays [18]. Here the effect arises from an increase in the effective wavevector of the radiation in the magneto-optically active medium.

Table 1 Nano-enhanced optical transitions. Enhancement of different electromagnetic quantities leads to enhancement of different types of molecular transitions. The references and examples given are intended to be illustrative rather than exhaustive.

Type of transition	Electromagnetic quantity enhanced	Spectroscopic quantity enhanced
Electric dipole absorption and emission [34,39,40]	$\langle \lvert\mathbf{E}\rvert^2 \rangle$	Excitation, fluorescence, and photochemistry (same spectrum as far-field)
Magnetic dipole absorption and emission [41,42]	$\langle \lvert\mathbf{B}\rvert^2 \rangle$	Excitation and emission from ''dark'' states; demonstrated in Lanthanide chelates
Electric dipole and electric quadrupole Raman scattering [21–23]	$\langle \lvert\mathbf{E}\rvert^2 \rangle$, $\nabla\mathbf{E}$	Surface-enhanced Raman scattering (SERS)
Electric dipole and electric quadrupole Raman optical activity [25,26,29]	$\langle \lvert\mathbf{E}\rvert^2 \rangle$, $\nabla\mathbf{E}$	Surface-enhanced Raman optical activity (SEROA)
Electric dipole–magnetic dipole interference [43]	$\langle \mathbf{E}\cdot\nabla\times\mathbf{E}\rangle = -\left\langle \mathbf{E}\cdot\frac{\partial\mathbf{B}}{\partial t}\right\rangle$	Circular dichroism
Magnetic quadrupole transitions [44]	$\langle \lvert\nabla\mathbf{B}\rvert^2 \rangle$	Intersystem crossing, leading to magneto-optic, magnetochemical, and magneto-electronic effects

Surface enhanced Raman scattering (SERS) is the most famous nano-enhanced spectroscopic effect. For a recent review see [19]. The Raman signal from molecules adsorbed on ''hot spots'' of gold or silver nanoparticles is enhanced by up to *12 orders of magnitude* relative to the signal from the same molecules in bulk [20]. Much theoretical effort has been devoted to explaining this phenomenon. The current consensus is that the effect arises through three mechanisms [21]: (1) enhanced strength of the input field at the location of the molecule; (2) enhanced coupling of the molecular transitions to the scattered field; and (3) a ''chemical interaction'' involving charge transfer between the molecule and the nanoparticle. The combination of the first two effects leads to a dependence on $|E|^4$, where E is the electric field strength at the location of the molecule.

Several authors have pointed out that part of the SERS enhancement may also arise from increased electric field gradients near a nanostructure. These gradients can lead to SERS through two distinct mechanisms: (1) quadrupolar contributions to virtual transitions between ground and electronically excited states [22] and (2) a ''gradient field Raman'' effect in which the electric gradient generates internal stresses in a molecule that lead to vibrational excitation [23]. SERS spectra often show different selection rules than bulk Raman spectra. Both of the gradient-enhanced mechanisms can account for these differences. Thus far there has been no unambiguous apportionment of SERS enhancements among the multiple possible contributing factors.

Raman optical activity (ROA) describes the difference in Raman signals from a chiral molecule subject to left- or right-circularly polarized light [24]. As with conventional circular dichroism, ROA signals are smaller than their achiral counterpart by a factor of $\sim 10^3$, due to the small size of a molecule relative to the wavelength of light. As with conventional Raman, there has been interest in using surface-enhanced Raman optical activity (SEROA) to generate larger signals. Metallic nanostructures can, in principle, enhance the ROA signal to an even greater degree than they enhance conventional Raman. This additional enhancement in SEROA arises through an interference between electric dipole and electric quadrupole contributions to the Raman scattering. While quadropole transitions are only weakly excited by far-field radiation, they can be strongly excited in oriented molecules near a metallic nanostructure. This effect was first predicted by Efrima in the 1980s [25,26], but in spite of continued theoretical work [27,28] has lacked experimental verification until recently [29].

The emphasis of this review is on enhanced optical excitation in sculpted fields. A related topic is enhanced spontaneous *emission* of molecules near nanostructures. The presence of a nanostructure may modulate the density of states into which a molecule may deposit its excitation energy, and thereby modulate the rate of spontaneous decay. Monolayers of dyes [30,31], and single molecules [32] have been sandwiched in optical cavities, placed near metal tips [33], or on metallic nanoparticles [34], leading to dramatic changes in excited state lifetime. The direction of emission of a single molecule can also be influenced by a proximal metallic ''nano antenna'' [35]. Novotny's book on Nano-Optics provides a nice discussion of such effects [36]. Also worth mentioning are experiments on fluorophores in liquid micro-droplets [37,38]. Here the liquid droplet forms a high Q resonant cavity and can dramatically enhance the rate of spontaneous emission of molecules contained within the cavity.

Chiral photochemistry with superhelical light

Chiral objects are bodies, such as a human hand, whose mirror image may not be superimposed on the original. Chirality is fundamental to life, as most biomolecules occur in only one chirality, and thus also to medicine, as a drug molecule and its mirror image may have drastically different pharmacological properties [45,46]. Opposite enantiomers (i.e. molecules with opposite chirality) are indistinguishable in most regards: all scalar physical properties (e.g. density, molecular weight, enthalpy of formation, electronic and vibrational frequencies) are identical. Reactivity with achiral compounds is also the same for both enantiomers. Only in their interactions with other chiral objects do enantiomers become distinguishable.

Circularly polarized light (CPL) is a chiral object, so its interactions with matter are sensitive to molecular chirality. In particular, the extinction coefficients are slightly different for propagation of CPL through solutions of opposite enantiomers, an effect known as circular dichroism (CD). The strength of this asymmetry is measured by the dissymmetry factor

$$g \equiv \frac{2(\Gamma^{+} - \Gamma^{-})}{(\Gamma^{+} + \Gamma^{-})},$$

where $\Gamma^{+/-}$ are the rates of excitation of a single enantiomer in right- and left-CPL, respectively (or equivalently, opposite enantiomers in light of a single handedness).

Over the nearly two centuries since the discovery of chiroptical phenomena, much effort has gone into predicting CD spectra from molecular models, and into inferring molecular structure from CD spectra. Today, circular dichroism measurement is a standard tool to characterize organic and biological compounds. However, typical g-values are very small ($<10^{-3}$). Small signals limit the accuracy of CD measurements, and lead to a requirement for large sample volumes. Therefore, there is good motivation to find generic mechanisms to enhance CD signals.

Circular dichroism is a small effect because of the mismatch between the wavelength of light and the molecular size [45]. Typical wavelengths are hundreds of times larger than molecular diameters, so the pitch of the electromagnetic helix in CPL is hardly discernable to the molecule sitting in the field. Put differently, chiroptical effects originate from interference between an electric dipole transition and a magnetic dipole transition [47]. For most molecules, the magnetic dipole transition moment is smaller than its electric counterpart by a factor of order R_{mol}/λ, so chirally sensitive transitions are much smaller than the achiral background.

A longstanding dream of synthetic chemists is to create chirality *de novo* [48,49]. In every chiral synthesis performed today, chirality is imparted to the product either from chiral starting materials, a chiral catalyst, or a chiral separation. These chiral building blocks all ultimately trace their origin to biogenic sources. However, it is in principle possible to impose a chiral bias on a reaction through an interaction with a chiral physical field, rather than a chiral molecule.

Circularly polarized light is one such chiral field that may impart a slight chiral bias to a photochemical reaction, an effect first demonstrated in 1929 by Kuhn and coworkers [50,51]. While CPL-driven chiral photochemistry has subsequently been observed many times (see, e.g. [52—54]), it has yet to become a practical tool because g-values are so small.

In recent years interest has shifted toward using nonlinear spectroscopy [55,56] and coherent control [57,58] to induce chiral transitions using light. Theoretical proposals have suggested that large enantiomeric excesses could be attained [45,59,60], but the experimental work has mostly been limited to simple model systems [60]. The design of pulses for coherent control of molecular chirality is still a daunting theoretical challenge, and any solution to this challenge is specific to a single type of molecule.

Even if one restricts consideration to continuous wave (CW) solutions to Maxwell's equations (i.e. solutions sinusoidally varying in time), CPL is just one of an infinite number of such solutions. Could there be CW solutions to Maxwell's equations that show greater enantioselectivity than do circularly polarized plane waves? One could imagine an electromagnetic field with a particularly large twist, which couples strongly to molecular chirality. Any such field is likely to require nanostructures to set the appropriate boundary conditions.

How does one quantify the chirality of the electromagnetic field? The concept of chirality of a vector field occurs in fluid dynamics [61], plasma physics [62], and in topological quantum field theory [63], but to our surprise we have not found a discussion of this concept in relation to optical spectroscopy. We invented a quantity which we call the electromagnetic chirality, which measures the local density of handedness, or twistiness, of the electromagnetic field [43]. In a chiral field, the field lines wrap around a central axis, but also have a component parallel to the axis. Based on this picture, we introduce a dimensionless pseudo-scalar relative chirality:

$$\eta \equiv \frac{c}{\omega} \frac{\langle \mathbf{E} \cdot \nabla \times \mathbf{E} \rangle}{\langle |\mathbf{E}|^2 \rangle} \tag{1}$$

where ω is the frequency, c the speed of light, and $\mathbf{E}$ the electric field; the brackets indicate an average over time. The factor of $\langle |\mathbf{E}|^2 \rangle$ in the denominator is for convenience and to make η dimensionless. The electromagnetic chirality should not be confused with the ''electromagnetic helicity'', which describes the polarization state within a single plane [64]. As conventionally defined, ''helicity'' refers to a two-dimensional property of the field while the new ''chirality'' which we introduce refers to a three-dimensional property.

Given an arbitrary time-dependent electromagnetic field, it is a simple matter to calculate the chirality at each point in space. The well known descriptors of an electromagnetic field are the energy density (a scalar), the Poynting vector (a vector), and the angular momentum (a pseudo-vector). The chirality (a pseudo-scalar) completes this quartet, and is a fundamental property of the electromagnetic field, at the same level as the other three descriptors. The relative chirality of a CPL plane wave is $\eta = \pm 1$.

Do molecules care about the electromagnetic chirality? Leon Rosenfeld's 1929 quantum mechanical derivation of circular dichroism [65] considered a chiral molecule subject to a circularly polarized plane wave. Subsequent treatments [47,66] followed this same scenario, albeit with more sophisticated handling of the molecule and the electromagnetic field. We redid the calculations in Rosenfeld's original paper, using time-dependent perturbation theory to calculate the response of a chiral molecule in a time-periodic electromagnetic field of *arbitrary* three-dimensional shape [43]. We found that the electromagnetic chirality is the quantity that couples to chirally sensitive molecular transitions. The g-value in an arbitrary electromagnetic field is related to its value in CPL by

$$g = \eta g^{\mathrm{CPL}}.$$

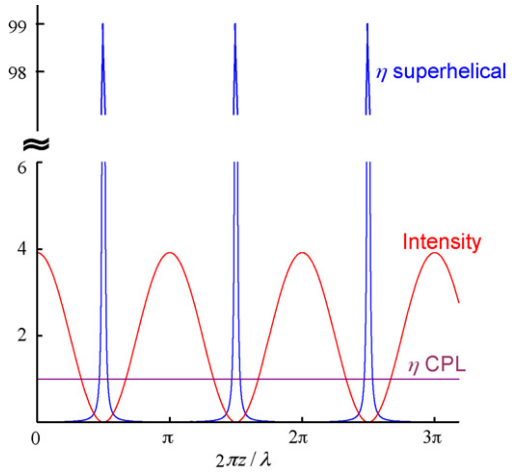

Figure 2 Helicity of a superhelical electromagnetic field. Blue: relative helicity in superhelical light. Purple: relative helicity in conventional circularly polarized light. Red: intensity distribution in superhelical light.

Thus one can enhance the dissymmetry factor, *g*, either by changing the structure of a molecule, *or* by tuning the electromagnetic chirality.

Do Maxwell's equations allow one to create electromagnetic fields in which the relative chirality is larger than for circularly polarized plane waves? We showed by explicit construction that the answer is yes. A ''superhelical'' field consists of two counter-propagating CPL plane waves, of the same frequency and phase, slightly different amplitude, and opposite handedness. Counter-propagating plane waves generate a standing wave of intensity (proportional to $\langle|\mathbf{E}|^2\rangle$), while, one can show, the term $\langle E\cdot\nabla\times E\rangle$ in Eq. (1) remains constant independent of position. Thus the relative chirality becomes large at a node in the standing wave. The two counter-propagating waves must have slightly different amplitude so that the overall field configuration remains chiral. If a racemic mixture of chiral molecules is confined near a node of a superhelical field, one enantiomer will be excited with far higher probability than the other. Fig. 2 shows the distributions of relative chirality and intensity in superhelical light.

Experimental tests of chiral photochemistry in superhelical light

Here we propose an experiment to test for enantioselective excitation in superhelical light. We present progress towards achieving the necessary conditions, although the predicted effect has not yet been observed. The general scheme of the experiment is shown in Fig. 3. A superhelical standing wave is set up by reflecting CPL off an imperfect mirror at normal incidence. An imperfect mirror has the convenient property of interchanging left- and right-CPL, while the reflected wave has slightly lower amplitude than the incident wave. Thus the interference of the incident and reflected waves generates a superhelical field. Molecules are confined to a thin plane at various points in the standing wave and their degree of excitation is recorded as a function of position and circular polarization state of the input light.

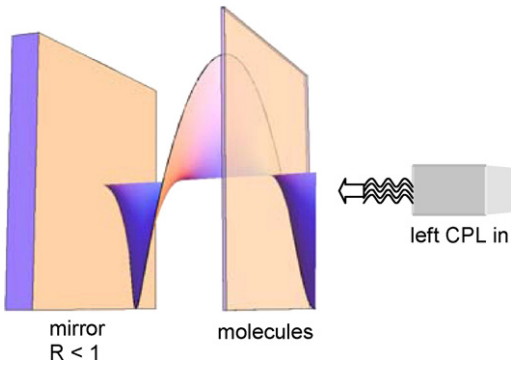

Figure 3 Schematic of an experiment in which molecules are confined at the nodes of a superhelical standing wave. A mechanical spacer must confine the molecules to a thin plane parallel to a reflective surface.

One challenge in these experiments is that the molecules must be confined to a plane that is thin relative to the wavelength of light, imposing a severe constraint on the number of molecules that can be probed. Absorption signals are proportional to optical path length, and thus would not be detectable on a monolayer of chiral molecules. We chose to use visible fluorescence to measure the degree to which chiral molecules are excited, i.e. to use fluorescence detected circular dichroism (FDCD). This technique provides much higher sensitivity than conventional CD.

The molecules currently under investigation are bridged triarylamine helicene—camphanate derivatives (H-1 and H-2 for two enantiomers). These chiral molecules were first reported by Field et al. [67], and were synthesized in an undergraduate organic chemistry class at Harvard. Both enantiomers show strong circular dichroism, and strong fluorescence (Fig. 4).

We propose to use an optical microscope to excite the chiral molecules and to detect their weak fluorescence. A chief pitfall in performing FDCD measurements in an optical microscope is contamination of the signal by *linear* dichroism, which is typically ~1000 times larger than the CD signal. Even if one sends perfect CPL into the microscope, slight linear birefringence and linear dichroism in the internal components can lead to elliptically polarized light at the sample, and to a spurious signal from linear dichroism.

To circumvent the problem of non-ideal optical elements, we developed the micro-patterning scheme shown in Fig. 5. We use microcontact printing to lay down alternating lines of chiral and achiral fluorophores. The achiral molecules form a built-in control for every measurement. As we switch between left and right superhelical light, any changes in the fluorescence intensity in the achiral molecules can be used to perform a background correction to the signal from the chiral molecules. Fig. 6b shows the result of this stamping procedure.

The superhelical standing wave is generated by reflecting CPL off an imperfect mirror mounted just above the patterned coverslip (Fig. 6). We mount the coverslip at a slight angle relative to the mirror, so that a single image of the coverslip records fluorophores at a range of *z*-coordinates along the standing wave. The vertical stripes in Fig. 6c are due to the standing wave from the mirror.

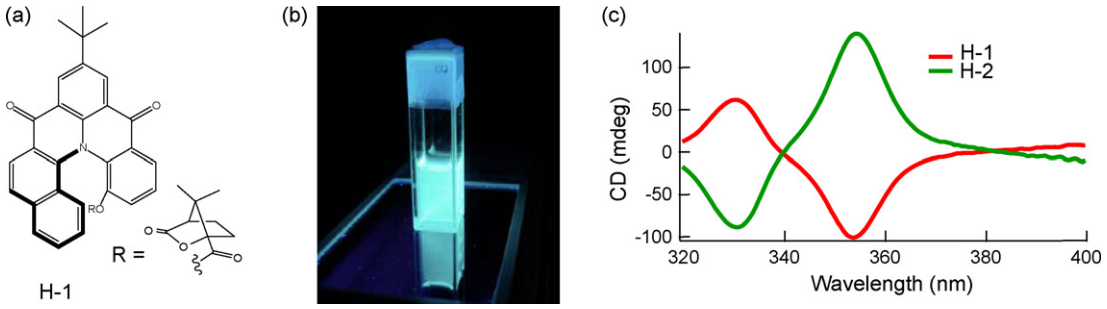

Figure 4 Molecules used to measure fluorescence detected circular dichroism (FDCD) in superhelical light. (a) Structure of the H-1 enantiomer. The camphanate group was used as a chiral resolving agent and rendered the H-1 and H-2 species technically diastereomers. However, the camphanate group had no detectable effect on the optical properties of either species. (b) Image of fluorescence acquired under ultraviolet illumination. (c) Circular dichroism spectra for opposite enantiomers, H-1 and H-2.

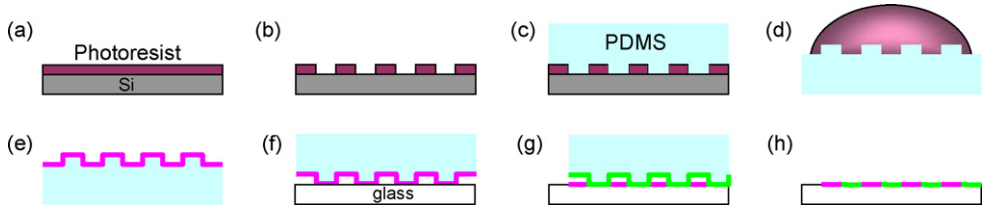

Figure 5 Microfabrication of alternating stripes of chiral and achiral fluorophores. (a–c) Formation of a poly(dimethyl siloxane) (PDMS) stamp by conventional photolithography followed by casting of PDMS. (d and e) Inking of the stamp with a solution of chiral fluorophores. (f) Transferring the pattern to a substrate via microcontact printing. (g and h) Repeating the process with achiral fluorophores.

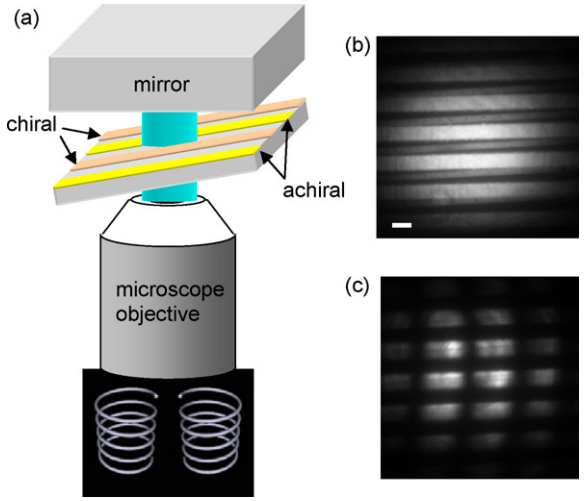

Figure 6 (a) Illumination scheme for detecting enantioselective excitation in a superhelical standing wave. Left- and right-CPL are alternately introduced into the microscope. A mirror mounted above the sample reflects the light to generate a superhelical standing wave. A coverslip patterned with chiral and achiral molecules is introduced at an angle relative to the mirror. (b) Fluorescence image without the top mirror, showing alternating chiral and achiral stripes (the chiral and achiral stripes are different widths so we can distinguish them). Scale bar 10 μm. (c) Fluorescence image with the top mirror, showing an optical standing wave (vertical stripes) superimposed on the patterned molecules (horizontal stripes).

Our optical setup is designed to illuminate the sample alternately with left- and right-CPL. This seemingly simple task is complicated by the birefringence and linear dichroism of the optical elements inside a fluorescence microscope. We measured the Jones matrix of each component (which determines its effect on the polarization of light). By inverting these matrices we determined the state of elliptical polarization to send into the microscope to generate circular polarization at the sample. We use a liquid crystal variable retarder to switch between left- and right-CPL and have automated the data collection so that thousands of images can be acquired in a single session. Current work is focused on optimizing the optical excitation and detection system.

Imaging of circular dichroism

As a preliminary proof-of-principle we imaged the CD of helicene using fluorescence (without any superhelical enhancement). To our knowledge, this experiment is the first demonstration of circular dichroism *imaging*. Our camera-based FDCD setup consists of a mercury arc lamp filtered to provide illumination at 355 nm, a polarizer, a rotating quarter wave plate to create alternately left- and right-CPL, and a high-sensitivity Electron-Multiplying CCD (Andor iXon$^+$) to record the images. One cuvette was filled with a racemic mixture of the helicenes, and a second cuvette was filled with a solution of a single enantiomer. The two cuvettes were put in series along the beam path; the racemic sample served as a built-in control to correct for imperfections in the optics and fluctuations in lamp intensity. Images were recorded under left- and right-CPL, first with H-1, then with H-2.

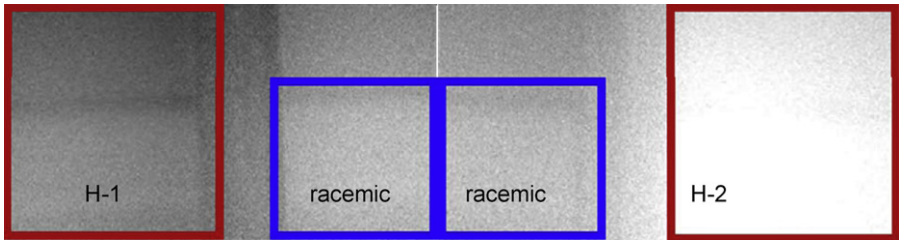

Figure 7 Fluorescence detected circular dichroism images of chiral helicenes, H-1 and H-2. The area in the two blue boxes is the racemic mixture; the regions in red boxes are H-1(left) and H-2(right).

The two chiral solutions (H-1 and H-2) looked indistinguishable to the eye in unpolarized room light. However, in the presence of CPL they showed detectably different fluorescence levels, with the sign of the difference depending on the helicity of the CPL. In Fig. 7 we display $I_L - I_R$ for both solutions, where $I_{L,R}$ is the intensity of fluorescence, normalized by the intensity of the racemic mixture, under left- or right-CPL.

With continued work in this area we hope soon to demonstrate that the electromagnetic field can be engineered to induce chirally selective transitions with enantioselectivity far larger than that can be achieved with circularly polarized light. We will work on pushing the effect further into the UV, to enhance the sensitivity to biological compounds which typically show strong CD at wavelengths <350 nm. Circular dichroism with superhelical light may provide a new ultrasensitive approach to characterizing biomolecules on surfaces.

Nanomagnetic catalysis

Now we turn to a second example of photochemical control with sculpted electromagnetic fields. We seek to address the question: can a weak magnetic field affect the outcome of a chemical reaction? At first blush this seems implausible: Zeeman splittings are so much smaller than thermal energy that any effects on equilibrium constants are imperceptibly small. Nonetheless magnetic field effects (MFE) have been observed in many nonequilibrium processes that go through a bi-radical intermediate [68—70]. The magnetic field is thought to affect the spin dynamics in the excited-state manifold, and thereby to determine the branching ratio between singlet and triplet reaction channels.

Here we briefly review the known mechanisms of MFE on photochemical reactions, and then propose a mechanism by which magnetic nanostructures can lead to dramatically larger effects. Electrons carry spin 1/2, so two electrons may exist in either a singlet or one of the three triplet states. The outcome of a reaction may depend on the spin multiplicity: singlet states are prone to recombine, while triplet states are forbidden from doing so by the Pauli Exclusion Principle and are more likely to react with other nearby species. The process of flipping between singlet and triplet states is called intersystem crossing (ISC). ISC involves a change in the parity of the spin wavefunction, and thus constitutes a *magnetic quadrupole* transition. Magnetic quadrupole transitions couple extraordinarily weakly to far-field radiation, so ISC is typically a slow process.

For well-separated electrons (i.e. a bi-radical), the singlet and three triplet states are all degenerate. At thermal equilibrium, all four states are populated with equal probability. Optical excitation, however, often generates bi-radicals in a pure spin state — either singlet or triplet — opening the door for weak magnetic fields to influence the outcome of the reaction.

An electronic spin in a magnetic field precesses about that field on the Bloch sphere at a Larmor frequency $\omega_L = g\mu_B B/\hbar$, where $\mu_B = 9.3 \times 10^{-24}$ J/T is the Bohr magneton, and the Landé g-factor of the electron is ≈2.002. ISC occurs in approximately the time it takes the two electrons to accumulate a relative phase shift of 180°:

$$\tau_{ISC}^{-1} \approx \frac{\mu_B}{\pi\hbar}(B\Delta g + g\Delta B), \tag{2}$$

where Δg is the difference in g-factor between the electrons and ΔB is the difference in local magnetic field. The g-factor differs from its free-space value because of local chemical interactions, and for organic molecules, $\Delta g \sim 10^{-3}$. Thus a homogeneous field of 1000 G induces ISC in 10^{-7} to 10^{-6} s. The rate of ISC is proportional to the magnetic field in this ''Δg mechanism'' [68]. Macroscopically generated fields are essentially constant over molecular dimensions, so for macroscopic fields $\Delta B = 0$.

A second source of ISC arises from hyperfine coupling between electronic spins and nearby magnetically active nuclei (^{1}H, ^{14}N, ^{13}C). This coupling leads to an effective magnetic field of 1—30 G, which is uncorrelated between the two electrons (they are coupled to different nuclei). The hyperfine field comes from randomly oriented nuclear spins, so it couples the singlet state with all three triplet states. An external field lifts the degeneracy of the triplet states, and suppresses the hyperfine field's ability to couple to the T_+ and T_- states. In contrast to the Δg mechanism, the hyperfine mechanism leads to a *decrease* in the rate of ISC with increasing magnetic field. The effect of an external field saturates when the field is much greater than the hyperfine field, so the hyperfine mechanism tends to dominate at low fields and the Δg mechanism dominates at high fields.

Magnetic field modulated ISC has been detected in the photoconductivity [71—73], photoluminescence [74], excited state lifetime [75,76], and chemical reactivity [68] of many molecular systems, and even in the dynamics of photosynthesis in plants [77]. Magnetic field effects on the reaction outcome are already known for dozens of photochemical processes. Model systems include electron transfer between pyrene and dimethylaniline [78] and in photolysis of benzophenone [79] and dibenzyl ketone [80,81]. MFE on polymerization have been observed in systems where the

initiator goes through a bi-radical [82,83]. Magnetic field modulation of bi-radical reactions is speculated to play a role in magnetic navigation in birds [84—86] and *Drosophila* [87], although this hypothesis remains unproved. Recently, MFE on spin dynamics in solid-state systems have attracted interest. In particular, semiconductor double-dots allow high resolution studies of ISC at low temperatures [88], and nitrogen-vacancy defects in diamond have been proposed as nanoscopic magnetometers [89].

Can we engineer the magnetic field to control ISC and thereby to control chemical processes? Examining Eq. (2) reveals that this is indeed possible if we can generate a magnetic field that changes significantly over the separation of the pair of spins. Typical bi-radicals in solution are separated by ~1 nm. The magnetic field gradient should overwhelm the effects of hyperfine fields, so we desire a gradient stronger than ~30 G/nm. Macroscopic coils cannot generate such gradients, but magnetic nanostructures, such as magnetic nanoparticles or ferromagnetic domain boundaries, can. The spirit of our proposal is similar to Wigner's mechanism for ortho—para nuclear conversion in H_2, in which collisions with paramagnetic ions lead to transient strong magnetic field gradients that cause nuclear ISC [90—92].

To illustrate the strength of field gradients near a magnetic nanostructure, we model a ferromagnetic nanoparticle as a uniformly magnetized sphere, with magnetic moment **m**. The magnetic field outside the sphere is the same as that of a point dipole of moment **m** located at the center of the sphere, and the field gradient $\nabla\mathbf{B}$ near the surface varies as the inverse of the radius of the particle. Small particles can generate enormously large gradients. For instance, a magnetically saturated sphere of Fe_3O_4 with a diameter of 10 nm generates a field gradient of about 600 G/nm at its surface. A similar argument applies to ferromagnetic domain boundaries, near which field gradients can approach 1000 G/nm. These magnetic field gradients can completely overwhelm hyperfine fields as a source of ISC in nearby molecules.

We illustrate the effect of this sculpted magnetic field on ISC in Fig. 8. Here we simulate the spin evolution of a radical pair, including the effects of magnetic field gradients near a nanoparticle, as well as local hyperfine fields. The hyperfine coupling constants correspond to the bi-radical formed from pyrene (Py) and dimethylaniline (DMA). This system is well known to show magnetic field effects on delayed fluorescence and has been thoroughly characterized in bulk [78,93—95].

In the absence of an external magnetic field, Fig. 8b shows that nuclear hyperfine effects lead to ISC in approximately 5 ns. Application of a modest uniform magnetic field of 500 G slows down ISC and also increases the quasi-steady state singlet probability. In this system the Δg effect is insignificant. The remarkable finding is that a steeply varying field due to a magnetic nanoparticle dramatically accelerates the rate of ISC. This enhancement of ISC can affect the outcome of the reaction, provided that the branching between singlet and triplet reaction channels occurs in <~5 ns. We therefore propose to use the sculpted fields near magnetic nanostructures to control the spin dynamics and the outcome of photochemical processes. This phenomenon is a form of heterogeneous catalysis that does not require molecular contact.

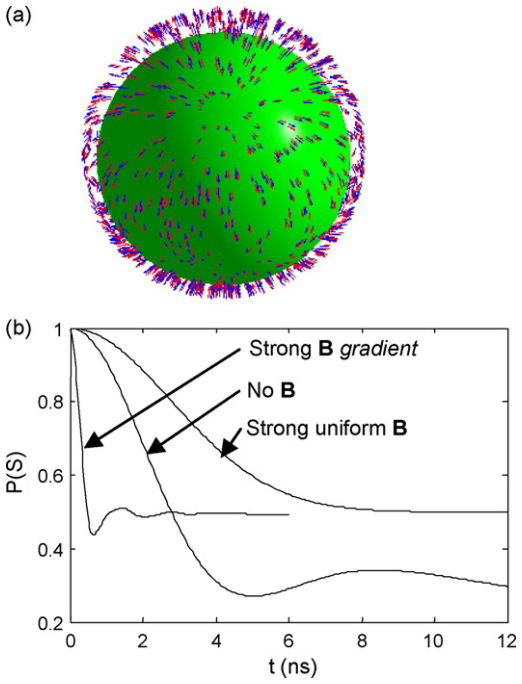

Figure 8 Intersystem crossing near a 20-nm diameter ferromagnetic nanocrystal. (a) Radical pairs distributed on the surface of the nanocrystal. Red and blue arrows represent the magnetic field from the nanoparticle at the location of the pyrene (Py) and dimethylaniline (DMA), respectively. (b) Singlet probability for Py/DMA radical ion pair, incorporating effects of hyperfine and inhomogeneous local magnetic fields.

We have considered a magnetic nanoparticle consisting of a single magnetic domain with a fixed orientation. The thermal environment could cause the magnetization to fluctuate. For a spherical particle, the time scale of this fluctuation is $\tau_{SPM} = \tau_0 e^{KV/k_BT}$, where τ_0 is a material-dependent attempt frequency, V is the volume of the nanoparticles, and K is the magnetocrystalline anisotropy. Particles above a threshold size have fixed magnetization on experimentally relevant timescales, while smaller particles fluctuate. In the limit $\tau_{SPM} \gg \tau_{ISC}$, the fluctuation has no effect on intersystem crossing. In the opposite limit $\tau_{ISC} \gg \tau_{SPM}$, the molecule sees an incoherently fluctuating magnetic field. Such a field still induces ISC, but at a rate that is slowed by an effect analogous to motional narrowing. For a semi-quantitative discussion of this regime see [44]. There are many materials for which nanoparticles may be large enough to be ferromagnetic at room temperature, but small enough to generate field gradients that dramatically enhance the rate of ISC. For example, a Fe_3O_4 nanoparticle of 8 nm radius has $\tau_{SPM} \sim 0.3$ s at room temperature. For such a particle we can ignore the effect of superparamagnetic fluctuations, yet we still find dramatically enhanced ISC.

To observe nanomagnetic catalysis experimentally, one needs to distinguish the effect from other interactions with the surface of the nanostructure. For instance, luminescence of organic molecules may be quenched by the surface of the magnetic material. Inert spacer layers can alleviate this problem, provided that the magnetic field gradient decays more slowly from the surface than does the quenching interaction. Non-optical readouts of ISC may also be

used. For instance, photolysis converts photoinitiators into spin-correlated radical pairs. The pair may either recombine or separate to release two free radicals into the solution. The most probable outcome depends on the relative rates of ISC and diffusional separation. Only the escape products can initiate radical polymerization reactions. This chemical detection scheme avoids the problem of quenching of luminescence by the surface.

Another challenge for experimental detection arises from the small volume of solution in which magnetic field gradients exist. An enhanced rate in a small fraction of the solution must compete with the un-enhanced process in the bulk. This problem may be alleviated by either working at high concentrations of magnetic nanoparticles, or by chemically immobilizing reactants near the surface of the nanoparticles.

Future prospects

We have discussed in detail two new ways to control matter with sculpted electromagnetic fields. Here we mention several other geometries worthy of exploration.

Purely magnetic dipole transitions can occur in molecular systems, but for most molecules these transitions are masked by their far stronger electric-dipole cousins. If one could generate an optical field in which all of the energy was in the magnetic field, then the magnetic-dipole transitions could be measured in the absence of the electric-dipole background.

Fig. 9a illustrates a simple nanostructure for generating such fields. A staircase pattern of transparent spacers is used to separate a monolayer of molecules from an aluminum mirror. These nanostructures are made using the photolithographic patterning scheme developed by Ajo-Franklin et al. [96], in which a staircase of 2^n steps requires only n rounds of photolithography and chemical vapor deposition. Fig. 9b shows some staircases of 64 steps, made with six rounds of processing. The colors result from thin-film interference from the differing step-heights.

Illumination of this nanostructure with linearly polarized monochromatic light at normal incidence produces an optical standing wave. Within this standing wave, a node in the electric field corresponds to an anti-node in the magnetic field. Molecules placed near electric nodes experience a purely magnetic field at the optical frequency—a situation that would be impossible to achieve with standard traveling waves. These molecules may undergo pure magnetic dipole-allowed transitions. Similar enhancements of magnetic dipole transitions have been predicted for spontaneous emission from molecules near reflecting films [41], and observed for the emission of lanthanide chelates near silver nanoparticles [42].

Other interesting geometries are shown in Fig. 9c and d. Sandwich nanostructures may be made of materials with dissimilar dielectric responses [97]. Molecules near the interface of these materials experience strong field gradients, even in the absence of strong absolute field strengths. Chiral nanostructures as shown schematically in Fig. 9d may also lead to highly twisted fields in their immediate vicinity.

Conclusion

The theory and experiments we propose here illustrate that one can use nanostructures to sculpt the electromagnetic field to induce highly non-trivial effects in molecules. Superhelical optical fields lead to strongly enhanced chiral asymmetry, while DC nanomagnetic field gradients lead to strongly enhanced intersystem crossing. Demonstrations of these effects may lead to new approaches to molecular control and to new nanostructured catalysts. Exploration of other spectroscopies in sculpted fields presents a largely open area for exploration. One can ask about the enhancement of nonlinear processes, the role of molecular motion and tumbling, and the effects of local fields near metamaterials, to name a few examples. Nanoscale sculpting of electromagnetic fields represents a new area of spectroscopic research with a bright future.

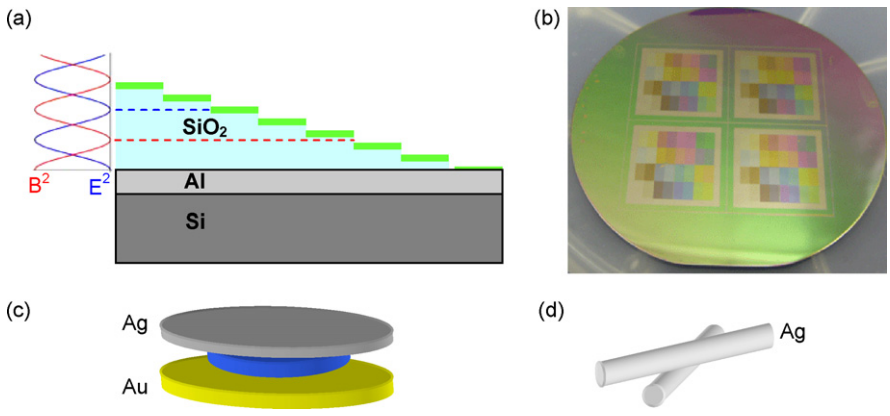

Figure 9 Nanostructures for spectroscopy in sculpted fields. (a) Staircase nanostructure for probing magnetically driven transitions. Schematic of the structure showing transparent steps of SiO_2 on a reflective backing. When illuminated with linearly polarized monochromatic light at normal incidence, some steps will reside in a node of either the electric field or the magnetic field. (b) Photograph of a device we made with 64 steps. (c) Sandwich nanostructure for generating strong field gradients. (d) Chiral nanostructure for generating highly twisted fields.

Acknowledgments

We thank Timothy Cook for synthesis of the helicenes H-1 and H-2. Thanks are due for the encouragement and financial support of this work by the MITRE Corporation and the U.S. Government's NanoEnabled Technology Initiative, a Dreyfus New Faculty Award, and the Office of Naval Research Young Investigator Program. This work was partially supported by the Materials Research Science and Engineering Center of the National Science Foundation under NSF Award Number DMR-02-13805, and the Harvard Center for Nanoscale Systems (CNS), a member of the National Nanotechnology Infrastructure Network (NNIN), which is supported by the National Science Foundation under award no. ECS-0335765.

References

[1] M. Aeschlimann, M. Bauer, D. Bayer, T. Brixner, F.J. Garcia de Abajo, W. Pfeiffer, et al., Nature 446 (2007) 301.
[2] T. Brixner, F.J. Garcia de Abajo, J. Schneider, W. Pfeiffer, Phys. Rev. Lett. 95 (2005) 093901.
[3] S. Mukamel, Principles of Nonlinear Optical Spectroscopy, Oxford University Press, USA, 1995.
[4] B.P. Krueger, G.D. Scholes, G.R. Fleming, J. Phys. Chem. B 102 (1998) 5378.
[5] U. Harbola, S. Mukamel, Phys. Rev. A 70 (2004) 52506.
[6] J. Hachmann, J.J. Dorando, M. Aviles, G.K. Chan, J. Chem. Phys. 127 (2007) 134309.
[7] M. Moskovits, Rev. Mod. Phys. 57 (1985) 783.
[8] A. Nitzan, L.E. Brus, J. Chem. Phys. 75 (1981) 2205.
[9] T. Liebermann, W. Knoll, Colloids Surf. A 171 (2000) 115.
[10] C.L. Haynes, R.P. Van Duyne, J. Phys. Chem. B 107 (2003) 7426.
[11] A. Sundaramurthy, P.J. Schuck, N.R. Conley, D.P. Fromm, G.S. Kino, W.E. Moerner, Nano Lett. 6 (2006) 355.
[12] E.J. Sánchez, L. Novotny, X.S. Xie, Phys. Rev. Lett. 82 (1999) 4014.
[13] I. Lieberman, G. Shemer, T. Fried, E.M. Kosower, G. Markovich, Angew. Chem. Int. Ed. 47 (2008) 4855.
[14] G. Shemer, O. Krichevski, G. Markovich, T. Molotsky, I. Lubitz, A.B. Kotlyar, J. Am. Chem. Soc. 128 (2006) 11006.
[15] P.M. Hui, D. Stroud, Appl. Phys. Lett. 50 (1987) 950.
[16] G. Shemer, G. Markovich, J. Phys. Chem. B 106 (2002) 9195.
[17] P.K. Jain, Y. Xiao, R. Walsworth, A.E. Cohen, Nano Lett. 9 (2009) 1644.
[18] G. Ctistis, E. Papaioannou, P. Patoka, J. Gutek, P. Fumagalli, M. Giersig, Nano Lett. 9 (2008) 1.
[19] P.L. Stiles, J.A. Dieringer, N.C. Shah, R.P. Van Duyne, Annu. Rev. Anal. Chem. 1 (2008) 601.
[20] S. Nie, S.R. Emory, Science 275 (1997) 1102.
[21] G.C. Schatz, Acc. Chem. Res. 17 (1984) 370.
[22] J.K. Sass, H. Neff, M. Moskovits, S. Holloway, J. Phys. Chem. 85 (1981) 621.
[23] E.J. Ayars, H.D. Hallen, C.L. Jahncke, Phys. Rev. Lett. 85 (2000) 4180.
[24] L.D. Barron, A.D. Buckingham, Mol. Phys. 20 (1971) 1111.
[25] S. Efrima, Chem. Phys. Lett. 102 (1983) 79.
[26] S. Efrima, J. Chem. Phys. 83 (1985) 1356.
[27] B.G. Janesko, G.E. Scuseria, J. Chem. Phys. 125 (2006) 124704.
[28] P. Bouř, J. Chem. Phys. 126 (2007) 136101.
[29] S. Abdali, E.W. Blanch, Chem. Soc. Rev. 37 (2008) 980.
[30] R.E. Kunz, W. Lukosz, Phys. Rev. B 21 (1980) 4814.
[31] M. Lieberherr, C. Fattinger, W. Lukosz, Surf. Sci. 189 (1987) 954.
[32] M. Steiner, F. Schleifenbaum, C. Stupperich, A. Virgilio Failla, A. Hartschuh, A.J. Meixner, ChemPhysChem 6 (2005).
[33] J.M. Gerton, L.A. Wade, G.A. Lessard, Z. Ma, S.R. Quake, Phys. Rev. Lett. 93 (2004) 180801.
[34] S. Kuhn, U. Hakanson, L. Rogobete, V. Sandoghdar, Phys. Rev. Lett. 97 (2006) 017402.
[35] T. Taminiau, F. Stefani, F. Segerink, N. Van Hulst, Nat. Photonics 2 (2008) 234.
[36] L. Novotny, B. Hecht, Principles of Nano-optics, Cambridge University Press, 2006.
[37] M.D. Barnes, C.Y. Kung, W.B. Whitten, J.M. Ramsey, S. Arnold, S. Holler, Phys. Rev. Lett. 76 (1996) 3931.
[38] A. Kiraz, A. Kurt, M.A. Dündar, A.L. Demirel, Appl. Phys. Lett. 89 (2006) 081118.
[39] P.J. Schuck, D.P. Fromm, A. Sundaramurthy, G.S. Kino, W.E. Moerner, Phys. Rev. Lett. 94 (2005) 7938.
[40] C.D. Geddes, J.R. Lakowicz, J. Fluoresc. 12 (2002) 121.
[41] W. Lukosz, R.E. Kunz, J. Opt. Soc. Am. 69 (1979) 1495.
[42] H. Nabika, S. Deki, Eur. Phys. J. D 24 (2003) 369.
[43] Y. Tang, A.E. Cohen (in preparation).
[44] A.E. Cohen (submitted).
[45] L.D. Barron, Molecular Light Scattering and Optical Activity, Cambridge University Press, 2004.
[46] N. Berova, K. Nakanishi, et al., Circular Dichroism: Principles and Applications, Wiley-VCH, 2000.
[47] D.P. Craig, T. Thirunamachandran, Molecular Quantum Electrodynamics, Courier Dover Publications, 1998.
[48] M. Avalos, R. Babiano, P. Cintas, J.L. Jimenez, J.C. Palacios, L.D. Barron, Chem. Rev. 98 (1998) 2391.
[49] L.D. Barron, J. Am. Chem. Soc. 108 (1986) 5539.
[50] W. Kuhn, E. Braun, Naturwissenschaften 17 (1929) 227.
[51] W. Kuhn, E. Knopf, Naturwissenschaften 18 (1930) 183.
[52] W.J. Bernstein, M. Calvin, Tetrahedron Lett. (1972) 2195.
[53] W.J. Bernstein, M. Calvin, O. Buchardt, J. Am. Chem. Soc. 94 (1972) 494.
[54] W.J. Bernstein, M. Calvin, O. Buchardt, J. Am. Chem. Soc. 95 (1973) 527.
[55] K. Hoki, L. González, Y. Fujimura, J. Chem. Phys. 116 (2002) 2433.
[56] K. Hoki, L. Gonzalez, Y. Fujimura, J. Chem. Phys. 116 (2002) 8799.
[57] M. Shapiro, P. Brumer, Rep. Prog. Phys. 66 (2003) 859.
[58] P. Brumer, E. Frishman, M. Shapiro, Phys. Rev. A 65 (2002) 015401.
[59] Y. Ma, A. Salam, Chem. Phys. 324 (2006) 367.
[60] T. Brixner, G. Krampert, T. Pfeifer, R. Selle, G. Gerber, M. Wollenhaupt, et al., Phys. Rev. Lett. 92 (2004) 208301.
[61] H.K. Moffatt, A. Tsinober, Annu. Rev. Fluid Mech. 24 (1992) 281.
[62] M.A. Berger, G.B. Field, J. Fluid Mech. 147 (1984) 133.
[63] A. Zee, Quantum Field Theory in a Nutshell, Princeton University Press, Princeton, NJ, 2005.
[64] V.B. Berestetskii, E.M. Lifshitz, et al., Quantum Electrodynamics, 2nd ed., Butterworth-Heinemann, 1982.
[65] L. Rosenfeld, Z. Phys. A: Hadrons Nucl. 52 (1929) 161.
[66] E.U. Condon, Rev. Mod. Phys. 9 (1937) 432.
[67] J.E. Field, T.J. Hill, D. Venkataraman, H. He, J.E. Janso, R.T. Williamson, et al., J. Org. Chem. 68 (2003) 6071.
[68] U.E. Steiner, T. Ulrich, Chem. Rev. 89 (1989) 51.
[69] N.J. Turro, Modern Molecular Photochemistry, University Science Books, 1991.
[70] S. Nagakura, H. Hayashi, et al., Dynamic Spin Chemistry: Magnetic Controls and Spin Dynamics of Chemical Reactions, Wiley-Kodansha, 1998.
[71] C. Boehme, K. Lips, Phys. Rev. B 68 (2003) 245105.
[72] D.R. McCamey, H.A. Seipel, S.Y. Paik, M.J. Walter, N.J. Borys, J.M. Lupton, et al., Nat. Mater. 7 (2008) 723.
[73] J.M. Lupton, C. Boehme, Nat. Mater. 7 (2008) 598.
[74] R.P. Groff, A. Suna, P. Avakian, R.E. Merrifield, Phys. Rev. B 9 (1974) 2655.

[75] P.W. Atkins, G.T. Evans, Mol. Phys. 29 (1975) 921.
[76] E.A. Weiss, M.A. Ratner, M.R. Wasielewski, J. Phys. Chem. A 107 (2003) 3639.
[77] C.E.D. Chidsey, L. Takiff, R.A. Goldstein, S.G. Boxer, Proc. Natl. Acad. Sci. U.S.A. 82 (1985) 6850.
[78] A. Weller, H. Staerk, R. Treichel, Faraday Discuss. Chem. Soc. 78 (1984) 271.
[79] Y. Fujiwara, T. Aoki, T. Haino, Y. Fukazawa, Y. Tanimoto, R. Nakagaki, et al., J. Phys. Chem. A 101 (1997) 6842.
[80] I. Rintoul, C. Wandrey, J. Polym. Sci. A 47 (2009) 373.
[81] M.A. Ushakova, A.V. Chernyshev, M.B. Taraban, A.K. Petrov, Eur. Polym. J. 39 (2003) 2301.
[82] I.V. Khudyakov, N. Arsu, S. Jockusch, N.J. Turro, Des. Monomers Polym. 6 (2003) 91.
[83] A.P. Chiriac, C.I. Simionescu, Prof. Polym. Sci. 25 (2000) 219.
[84] T. Ritz, S. Adem, K. Schulten, Biophys. J. 78 (2000) 707.
[85] H. Mouritsen, T. Ritz, Curr. Opin. Neurobiol. 15 (2005) 406.
[86] C.T. Rodgers, P.J. Hore, Proc. Natl. Acad. Sci. U.S.A. 106 (2009) 353.
[87] R.J. Gegear, A. Casselman, S. Waddell, S.M. Reppert, Nature 454 (2008) 1014.
[88] J.R. Petta, A.C. Johnson, J.M. Taylor, E.A. Laird, A. Yacoby, M.D. Lukin, et al., Science 309 (2005) 2180.
[89] J.R. Maze, P.L. Stanwix, J.S. Hodges, S. Hong, J.M. Taylor, P. Cappellaro, et al., Nature 455 (2008) 644.
[90] E. Wigner, Z. Phys. Chem. B 23 (1933) 28—32.
[91] K.G. Petzinger, D.J. Scalapino, Phys. Rev. B 8 (1973) 266.
[92] P. Atkins, M. Clugston, Mol. Phys. 27 (1974) 1619.
[93] A. Weller, F. Nolting, H. Staerk, Chem. Phys. Lett. 96 (1983) 24.
[94] A. Weller, H. Staerk, R. Treichel, Faraday Discuss. 78 (1984) 271.
[95] H. Staerk, W. Kuhnle, R. Treichel, A. Weller, Chem. Phys. Lett. 118 (1985) 19.
[96] C.M. Ajo-Franklin, C. Yoshina-Ishii, S.G. Boxer, Langmuir 21 (2005) 4976.
[97] T. Pakizeh, M.S. Abrishamian, N. Granpayeh, A. Dmitriev, M. Käll, Opt. Express 14 (2006) 8240.

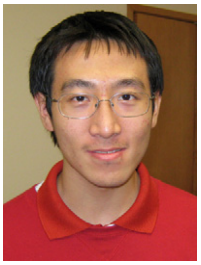

Nan Yang was born in Beijing, China. He obtained his B.A.Sc. from the Engineering Science program at University of Toronto, Canada. He is currently a graduate student at Harvard University, in the Cohen lab in the department of Chemistry and Chemical Biology. He is working on experimentally verifying some of the effects of nanomagnetic catalysis as discussed in this review.

Yiqiao Tang, born in 1984, obtained his bachelor degree in physics from Peking University (2007), with a research emphasis on generation and detection of spin-dependent photocurrent in semiconductor heterostructures. He entered the Physics Department at Harvard University with a Purcell fellowship in 2007, and joined Prof. Cohen's group in the same year. His current research focuses on engineering the electromagnetic field to enhance chiroptical effects in chiral molecules.

Adam Cohen graduated *summa cum laude* from Harvard College (2001) with an AB in chemistry and physics. From 2001 to 2003 he studied on a Marshall Scholarship at Cambridge, UK, where he obtained a PhD in theoretical physics, working on problems of biomechanics, intermolecular forces, and nonlinear spectroscopy. He then went to Stanford and obtained a second PhD in experimental physics. At Stanford, he invented the Anti-Brownian Electrokinetic trap (ABEL trap), a machine capable of trapping and manipulating individual biomolecules in solution. In 2007 he joined the Harvard faculty as an assistant professor of chemistry and chemical biology and of physics. Current research in the Cohen Lab focuses on the intersection of nanotechnology, biology, and quantum mechanics.